Laser-photodetachment of negative ions in He/O_2 barrier discharges

R. Tschiersch, S. Nemschokmichal and J. Meichsner

Institute of Physics, University of Greifswald, Felix-Hausdorff-Str. 6, 17489 Greifswald, Germany

Photodetachment experiments were performed in a glow-like He/O_2 barrier discharge. A Nd:YAG laser is used for the photodetachment of solely O_2^- at the fundamental wavelength, and of O^-, O_2^- as well as O_3^- by means of the second harmonic wavelength. The laser light caused a temporal shift of the discharge ignition to earlier times exclusively when firing the laser during the Townsend pre-phase. This can be explained by the photodetachment of negative ions: Detached electrons support the pre-ionization dynamics. The saturation of this effect in dependence on the laser pulse energy provides information about the predominance of the different negative ion species.

1 Introduction

Atmospheric pressure barrier discharges (BDs) have a high technological potential. In plasma chemistry and biomedicine, a crucial role is assigned to BDs operated in gas systems containing oxygen as an effective source of radicals. When admixing oxygen to a buffer gas like helium, the power requirement is low and the gas temperature is maintained close to room temperature. This is advantageous for the treatment of temperature-sensitive biological samples [1].

In the context of industrial applications, especially diffuse BDs generating non-thermal plasmas are of great interest. The helium BD is typically operated in the diffuse glow mode. When admixing oxygen, electron attachment processes become important which may significantly change the discharge properties.

As known from extensive investigations on low pressure discharges, the presence of electronegative components can strongly influence the discharge characteristics. The electron attachment to an electronegative species disturbs the ionization kinetics by diminishing the electron density. As well, the resulting negative ions enhance the ion-ion recombination. This can further lead to attachment-induced instabilities and discharge mode transitions [2, 3].

Unlike the comprehensive studies at low gas pressures, there is still a lag of experimental efforts in the field of atmospheric pressure discharges. Especially the small discharge dimensions down to the submillimeter scale are a great challenge for plasma diagnostics. Although numerical simulations often consider negative ions as one part of the charged particles balance [4], however, their role for the discharge development is not clearly emphasized.

The presented work investigates the significance of the electron attachment to oxygen in a glow-like He/O_2 barrier discharge by drawing conclusions from a laser-photodetachment experiment.

2 Experimental setup

Figure 1 illustrates the concentric discharge cell configuration. Both plane electrodes are covered with float glass (thickness $d_{gs} = 0.7\,\text{mm}$, dielectric constant $\varepsilon_{gs} = 7.6$) whereby a symmetrical discharge configuration is created. Four orifices enable the gas supply into the discharge volume, the investigation of the discharge emission, and the laser application. The experimental setup is shown in Figure 2.

The discharge cell is placed within a vacuum chamber which is pumped to a base pressure below $10^{-5}\,\text{mbar}$. Two mass flow controllers (1000 sccm and 1 sccm) handle the inlet of helium and oxygen (respective purity > 99.999 %). Well-defined He/O_2 mixtures are used with a maximum O_2 concentration of 1000 ppm. The operating pressure of 500 mbar is kept constant in the flowing regime ($F = 300\,\text{sccm}$).

A power supply operates the discharge by means of a sine wave feeding voltage ($f = 2\,\text{kHz}$). The transported charge $Q_{ext}(t)$ is measured via a capacitance ($C_{ext} = 1\,\text{nF}$) at the grounded electrode. As well, the total discharge current $I_{ext}(t)$ can be recorded via a resistor ($R_{ext} = 100\,\Omega$) instead of the capacitance. The discharge-induced current $I_{dis}(t)$ and the voltage drop across the gas gap $U_{gap}(t)$ are recalculated from the measured external quantities.

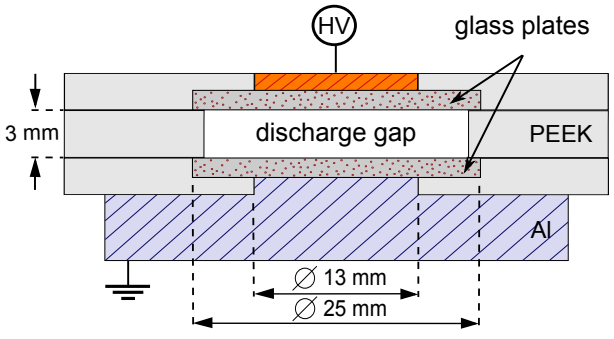

Fig. 1: Side-view of the discharge cell.

Spatio-temporally and spectrally resolved measurements of the discharge emission are performed by means of a moveable focusing lens, a monochromator (Acton Research Corporation, SpectraPro, focal length of 500 mm), and a photomultiplier tube (Hamamatsu R928). Thereby, the discharge gap is scanned with a spatial resolution of 0.1 mm at a maximum spectral resolution of 1 nm. The optical emission is processed into an electrical signal which is recorded by an oscilloscope (LeCroy 9362) and synchronized with the phase of the feeding voltage.

A Nd:YAG laser (Quanta Ray GCR 130, repetition rate of 10 Hz, maximum pulse energy of 170 mJ, beam wide of 9 mm) is used for the photodetachment experiment. At the fundamental wavelength $\lambda_L = 1064$ nm solely the detachment of O_2^- is possible, whereas at the second harmonic wavelength $\lambda_L = 532$ nm the three species O^-, O_2^-, and O_3^- are detached.

The laser beam is guided trough the discharge volume by means of a moveable optical system. A cylindrical lens focuses the beam only in its vertical extent down to 0.25 mm at the focal point (Gaussian beam optics). The latter can be shifted along the optical axis which allows the adjustment of the vertical beam extent within the discharge cell. Thereby, a large overlap between the laser beam and the discharge volume is achieved. In order to avoid the interaction between laser photons and the electrodes, the vertical beam extent is chosen to be approximately 1 mm. Behind the vacuum chamber, a power meter is mounted for the measurement of the laser pulse energy. At last, the laser pulse can be shifted along the phase of the feeding voltage by means of a pulse delay generator.

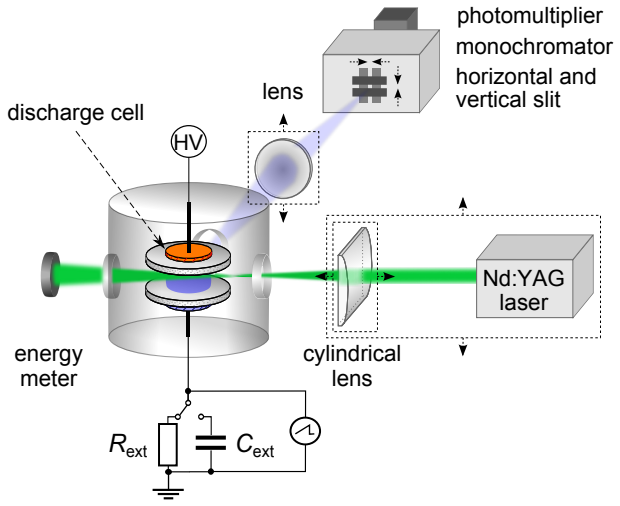

Fig. 2: Diagnostic setup: Electrical measurements, optical emission spectroscopy, and laser-photodetachment.

3 Barrier discharge in He/O_2 mixtures

Figure 3 illustrates an example for the barrier discharge in helium with small admixture (400 ppm) of oxygen, as typical for the studied operating conditions. The gap voltage $U_{gap}(t)$ and the discharge current $I_{dis}(t)$ are shown for one discharge cycle (T = 500 µs). Moreover, the spatio-temporally resolved radiation emission of the He line at $\lambda = 706$ nm is depicted. Two discharge breakdowns per half-period can be identified and must be distinguished.

The first breakdown is characterized by a large current amplitude at a short pulse duration, and by a significant drop of the gap voltage. Beyond, an intensive cathode-directed development of the He I emission is observed resulting in its maximum near the cathode. The latter indicates an ionizing front generating the typical axial structure of a glow-like barrier discharge [5]. In contrast, the current amplitude and the gap voltage drop of the subsequent breakdown is about one order of magnitude smaller. Most striking is the maximum radiation emission in front of the anode revealing the Townsend mode of the barrier discharge.

In general, with increasing admixture of oxygen to helium the discharge becomes more unstable and less intensive. A decrease in the charge amount transported during the breakdown is observed as well as a temporal jitter when comparing subsequent operating cycles. Most likely, these discharge instabilities can be explained by fluctuations in the electron density due to the electron attachment to oxygen, as already known from low pressure discharges.

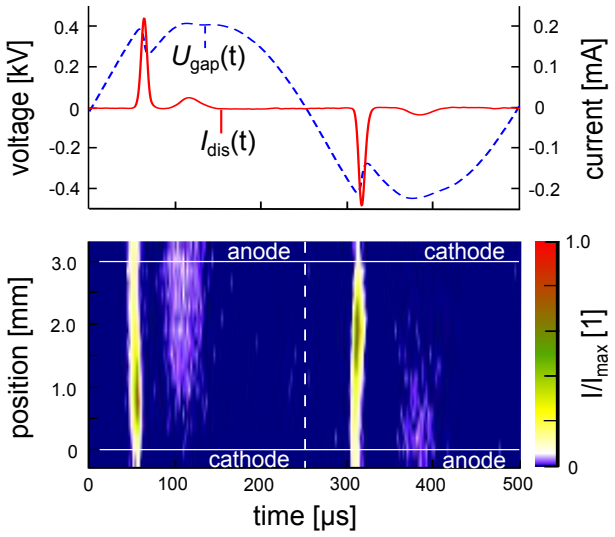

Fig. 3: Barrier discharge in He with 400 ppm O_2 admixture: Discharge current $I_{dis}(t)$ and gap voltage $U_{gap}(t)$, and discharge emission of He line at $\lambda = 706$ nm over one discharge cycle, $U_{app} = 0.8$ kV.

4 Photodetachment experiment

Control measurements are necessary in order to exclude undesirable laser-induced effects on the discharge, such as a significant interaction between laser photons and the dielectrics or the buffer gas helium. Therefore, the axial laser position was varied without hitting the charged dielectrics. As well, the laser pulse was shifted along the discharge cycle when operating the BD without any oxygen admixtures.

In figure 4, the gap voltage $U_{\mathrm{gap}}(t)$ and the discharge current $I_{\mathrm{dis}}(t)$ are presented for the laser-disturbed discharge in pure helium (above) and in helium with 600 ppm nitrogen admixture (center). The arrow marks the moment of the laser pulse. The laser wavelength is $\lambda_{\mathrm{L}} = 532\,\mathrm{nm}$ and the laser energy is maximal ($E_{\mathrm{L}} = 65\,\mathrm{mJ}$). In addition, the undisturbed electrical quantities are gray colored in the backround.

For each varied axial position and moment of the laser pulse, absolutely no change in the discharge development due to the laser application is observed at all. In conclusion, there is no significant laser-induced disturbance of the plasma chemistry in helium and He/N_2 mixtures. This result serves as a reference for the photodetachment experiment in He/O_2 mixtures.

In figure 4, an accordant measurement is shown for the discharge in helium with 400 ppm oxygen admixture (below). In contrast to the result in pure helium, a global effect on the discharge breakdown is observed, when firing the laser during the Townsend pre-phase (the related temporal window is blue colored).

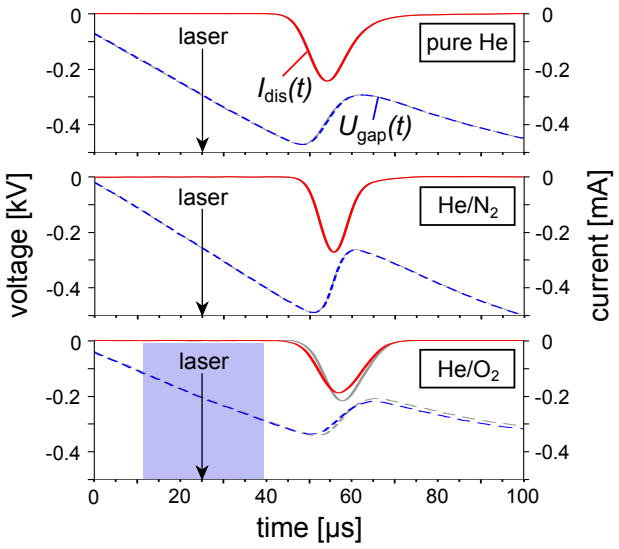

Fig. 4: Laser-disturbed discharge: Control measurements in pure He and He with 600 ppm N_2 admixture, and photodetachment effect in He with 400 ppm O_2. Voltage and current of the undisturbed discharge are gray colored in the background, $U_{\mathrm{app}} = 0.7\,\mathrm{kV}$, $\lambda_{\mathrm{L}} = 532\,\mathrm{nm}$.

The laser-affected discharge ignition is shifted by Δt to earlier times. Moreover, the transported charge during the discharge breakdown is diminished by ΔQ in comparison to the undisturbed situation. During the Townsend pre-phase, a low ionization rate at a small reduced electric field strength E/n leads to a slight increase in the charge carrier density. Under these conditions electron attachment processes become important. Hence, additional electrons produced by the laser-photodetachment of negative ions support the pre-ionization. In contrast, there is no change in the discharge properties, when firing the laser during the discharge breakdown. At large values of E/n, electron impact ionization and Penning ionization are dominant and electron attachment is negligible [6].

Figure 5 shows the characteristics Δt and ΔQ of the photodetachment effect in response to the laser pulse energy. As one can see, both quantities reached approximately saturation at $E_{\mathrm{L}} = 60\,\mathrm{mJ}$. When discussing the laser-induced effect on the He/O_2 discharge based on the photodetachment of negative ions, the maximum disturbance should be achieved at a maximum photodetachment efficiency. This is the case if all negative ions are detached within the discharge volume element which overlaps with the laser beam. With increasing laser pulse energy E_{L} at a constant laser profile A_{L}, the photodetachment efficiency

$$\frac{[\Delta e^-]}{[X^-]} = 1 - \exp\left(\frac{\sigma(E_{\mathrm{Ph}})}{E_{\mathrm{Ph}}} \cdot \frac{E_{\mathrm{L}}}{A_{\mathrm{L}}}\right), \qquad (1)$$

draws a saturation curve as well [7]. $[\Delta e^-]$ and $[X^-]$ denote the density of the detached electrons and the negative ions, respectively, E_{Ph} is the laser photon energy and $\sigma(E_{\mathrm{Ph}})$ is the photodetachment cross section.

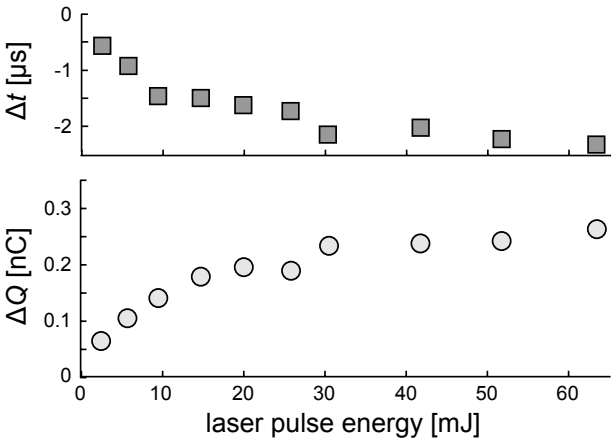

Fig. 5: Photodetachment effect in response to the laser pulse energy: Saturation curves for the temporal shift Δt of the discharge ignition and the less transported charge ΔQ.

In general, X^- includes the species O^-, O_2^-, and O_3^- formed by dissociative electron attachment

$$O_2 + e \rightarrow O^- + O, \quad (2)$$

or in termolecular reactions with the buffer gas helium

$$X + e + He \rightarrow X^- + He. \quad (3)$$

The three-body collison can be dominant at atmospheric pressure. When using the laser wavelength $\lambda_L = 532\,nm$, photodetachment of O^-, O_2^-, and O_3^- (i-−iii) must be considered as well as photodissociation of O_3^- generating O^- (iv), in turn followed by the photodetachment of O^-. The respective cross sections are given by (i) 6.4 ± 0.6, (ii) 1.2 ± 0.2, (iii) 0.2 ± 0.1, and (iv) 3.5 ± 0.5 in units of $10^{18}\,cm^2$ [8–11].

In figure 6, the laser-induced shift Δt of the discharge ignition and the less transported charge ΔQ are normalized to their fitted maxima from figure 5 and compared with the photodetachment efficiency of O^-, O_2^-, and O_3^- according to equation (1). As already discussed, these are corresponding quantities: The photodetachment efficiency directly determines and limits the observed effect on the discharge ignition. Due to the apparent agreement in figure 6, the laser-induced effect on the discharge seems to be mainly caused by the photodetachment of O_2^-.

But when selecting the detachment of solely O_2^- at the laser wavelength $\lambda_L = 1064\,nm$, the induced change in the discharge properties is near to the detection limit. In conclusion, the contribution of O_2^- to the overall negative ion density is negligible. Instead, the dominant species are O^- and O_3^-. To get a deeper inside into the influence of the photodetachment of negative ions on the He/O_2 barrier discharge, numerical simulations are necessary.

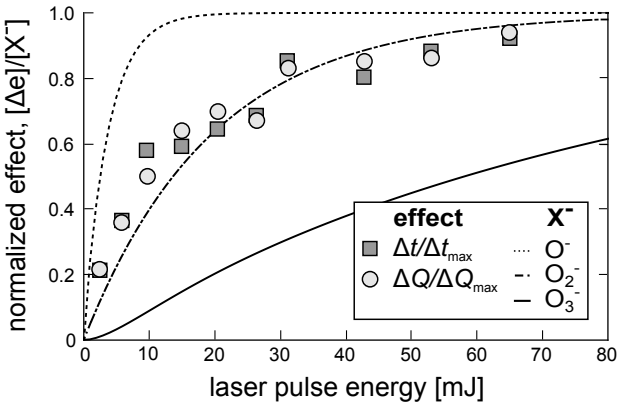

Fig. 6: Normalized effect $\Delta t/\Delta t_{max}$ and $\Delta Q/\Delta Q_{max}$, and photodetachment efficiency $[\Delta e]/[X^-]$ for different negative ion species X^- depending on the laser pulse energy.

5 Summary and outlook

The photodetachment of negative ions causes a global effect on the discharge breakdown of the glow-like He/O_2 barrier discharge solely when firing the laser during the Townsend pre-phase. Primarily, the discharge ignition is shifted to earlier times. The (few) detached electrons drive on the ionization dynamics which can be remarkable at comparably low charge carrier densities, such as during the discharge pre-phase. This behavior reaches saturation with increasing laser pulse energy, similar to the theoretical efficiency of the photodetachment of negative ions. To be able to determine the contribution of the different negative ion species, a numerical simulation is planned. Beyond, the investigation of other BD modes in electronegative systems will be a task for the future. Especially in the microdischarge regime, the radius of the filamentary breakdown channels might change in the presence of slow negative ions. In this context, the surface charge distribution as the footprint of a microdischarge channel will be studied by means of the electro-optic Pockels effect.

This work was supported by Deutsche Forschungsgemeinschaft, SFB TR 24.

References

[1] D. X. Liu, M. Z. Rong, X. H. Wang, F. Iza, M. G. Kong and P. Bruggeman *Plasma Process. Polym.* **7** (2010) 846 – 65

[2] H.-M. Katsch, A. Goehlich, T. Kawetzki, E. Quandt and H.-F. Döbele *Appl. Phys. Lett.* **75** (1999) 2023 – 5

[3] K. Dittmann, C. Küllig and J. Meichsner *Plasma Phys. Control. Fusion* **54** (2012) 124038

[4] D. Lee, J. M. Park, S. H. Hong and Y. Kim *IEEE Trans. Plasma Sci.* **33** (2005) 949 – 57

[5] F. Massines, A. Rabehi, P. Decomps, R. B. Gadri, P. Ségur and C. Mayoux *J. Appl. Phys.* **83** (1998) 2950

[6] K. Niemi, J. Waskoenig, N. Sadeghi, T. Gans and D. O'Connell *Plasma Sources Sci. Technol.* **20** (2011) 055005

[7] M. Bacal *Rev. Sci. Instrum.* **71** (2000) 3981 – 4006

[8] L. M. Branscomb, D. S. Burch, S. J. Smith and S. Geltman *Phys. Rev.* **111** (1958) 504 – 13

[9] D. S. Burch, S. J. Smith and L. M. Branscomb *Phys. Rev.* **112** (1958) 171 – 5

[10] L. J. Wang, S. B. Woo and E. M. Helmy *Phys. Rev. A* **35** (1986) 759 – 63

[11] P. C. Cosby, J. T. Moseley, J. R. Peterson and J. H. Ling *J. Chem. Phys.* **69** (1978) 2771 – 8